Author Manuscript

Author Manuscript

Author Manuscript

Author Manuscript

HHS Public Access

Author manuscript

Mucosal Immunol. Author manuscript; available in PMC 2019 May 29.

Published in final edited form as:

Mucosal Immunol. 2019 March ; 12(2): 518–530. doi:10.1038/s41385-018-0106-4.

CCR2 mediates increased susceptibility to post-H1N1 bacterial pneumonia by limiting dendritic cell induction of IL-17

Stephen J. Gurczynski[1], **Niket Nathani**[1], **Helen I. Warheit-Niemi**[2], **Elissa M. Hult**[2], **Amy Podsiad**[1], **Jane Deng**[1,3], **Rachel L. Zemans**[1], **Urvashi Bhan**[1,4], and **Bethany B. Moore**[1,2,*]

[1]Division of Pulmonary and Critical Care Medicine, Department of Internal Medicine, University of Michigan Medical Center, MI 48109

[2]Program in Biomedical Sciences, University of Michigan, 48109

[3]Veteran's Affairs Administration, Ann Arbor, MI 48109

[4]St. Joseph Hospital, Ypsilanti, MI 48197

Abstract

Post Influenza bacterial pneumonia is associated with significant mortality and morbidity. Dendritic cells (DCs) play a crucial role in host defense against bacterial pneumonia, but their contribution to post influenza-susceptibility to secondary bacterial pneumonia is incompletely understood. WT and CCR2$^{-/-}$ mice were infected with 100 plaque forming units (pfu) H1N1 intranasally alone or were challenged on day 5 with 7×10^7 colony forming units (cfu) methicillin-resistant *Staphylococcus aureus* intratracheally. WT mice express abundant CCL2 mRNA and protein post-H1N1 alone or dual infection. CCR2$^{-/-}$ mice had significantly higher survival as compared to WT mice, associated with significantly improved bacterial clearance at 24 and 48 hours (10 fold and 14 fold, respectively) post-bacterial challenge. There was robust upregulation of IL-23 and IL-17 as well as down-regulation of IL-27 expression in CCR2$^{-/-}$ mice following sequential infection as compared to WT mice, which was also associated with significantly greater accumulation of CD103$^+$ DC. Finally, WT mice treated with a CCR2 inhibitor showed improved bacterial clearance in association with similar cytokine profiles as CCR2$^{-/-}$ mice. Thus, CCR2 significantly contributes to increased susceptibility to bacterial infection after influenza pneumonia likely via altered dendritic cell responses and thus, CCR2 antagonism represents a potential therapeutic strategy.

Keywords

chemokine; IL-17; dendritic cells

Users may view, print, copy, and download text and data-mine the content in such documents, for the purposes of academic research, subject always to the full Conditions of use:http://www.nature.com/authors/editorial_policies/license.html#terms

*Corresponding author: Bethany B. Moore, University of Michigan Medical Center, Division of Pulmonary and Critical Care Medicine, 109 Zina Pitcher Place, 4053 BSRB, Ann Arbor, MI 48109-2200, Phone: (734) 647-8378, Fax: (734) 615-2331, bmoore@umich.edu.

Author Contributions

SJG, NN, HIWN, EMH, RLZ and AP performed experiments. SJG, RLZ, JD, BBM, and UB designed experiments, analyzed and interpreted data. SJG and NN wrote the manuscript. SJG, BBM, and JD edited the manuscript.

Author Manuscript Author Manuscript Author Manuscript Author Manuscript

Introduction

Seasonal Influenza A virus results in significant morbidity and mortality every year. In the United States alone, the Centers for Disease Control and Prevention estimate that seasonal influenza has been responsible for over 35 million cases, up to 710,000 hospitalizations and 56,000 deaths since 2010 (https://www.cdc.gov/flu/about/disease/2015-16.htm). In 2009, mortality reached pandemic levels, and the 2017 influenza season was also quite severe[1]. Antigenic drift and shift of hemagglutinin and neuraminidase are mechanisms for influenza to evade protective memory immune responses from prior exposure or vaccination[2] and thus, innate immunity is paramount for host protection.

Mortality from influenza is often due to secondary bacterial pneumonia with pathogens such as *Streptococcus pneumoniae* and *Staphylococcus aureus* as well as from the resulting inflammatory response as opposed to overwhelming viral replication[3]. In the 2009 H1N1 epidemic, infection with methicillin-resistant *Staphylococcus aureus* (MRSA) was a major bacterial complication[4]. Mounting evidence suggests that influenza modulates the innate immune response[2,5]. Recruitment of key innate immune cells, including monocyte-derived dendritic cells (DC) and macrophages to the lung is mediated via CC chemokine receptor 2 (CCR2). CCR2's interaction with its high-affinity ligand, CCL2, is an essential mechanism for monocyte cell trafficking from bone marrow to sites of inflammation[6]. Early cytokine / chemokine dysregulation including elevated CCL2 protein levels in bronchoalveolar lavage (BAL) fluid are found in mouse models of influenza pneumonia and have been associated with the accumulation of $CCR2^+$ monocytes, macrophages, and NK cells[7,8]. Additionaly, $CCR2^+$ cells have been suggested to contribute to lung injury and mortality in murine single infection influenza pneumonia models[8–10]. However, $CCR2^+$ cells are also believed to be important for clearance of bacterial pathogens in many settings[11–14]. Thus, it is difficult to predict how CCR2 function may ultimately impact disease outcomes in the setting of secondary bacterial infection post-influenza.

Previous studies have shown the importance of IL-17 in promoting bacterial clearance post-influenza and IL-17 is also important for clearance of MRSA[15–18]. Antigen presenting cells (APCs) in the lung produce IL-1β and IL-23 in response to various inflammatory stimuli and these cytokines activate STAT3-mediated transcription of IL-17 and IL-22, promoting differentiation of T-cells, neutrophil recruitment, and antimicrobial peptide production[19–21]. In mouse models of influenza pneumonia, expression of IL-1β and IL-23 as well as the downstream cytokines IL-17 and IL-22 are reduced[16, 22]. Furthermore, infection with influenza can directly suppress IL-17 production through up-regulation of miR-155[23]. As a result, initial infection by influenza virus exacerbates bacterial pneumonia[16, 24, 25]. The exact mechanism of how $CCR2^+$ leukocytes and IL-17 intersect to control immunity in the setting of post-influenza pneumonia is not known. However, we previously reported that loss of $CCR2^+$ monocyte recruitment enhanced IL-17 responses to γ-herpesviruses[26], and thus we hypothesized that loss of CCR2 signaling would promote IL-17 responses and improve bacterial clearance following influenza infection.

With this study, we identify CCR2 as a critical inhibitor of host immune responses post sequential pneumonia. Mice deficient in CCR2 ($CCR2^{-/-}$) had significantly improved

Author Manuscript Author Manuscript Author Manuscript Author Manuscript

mortality and improved bacterial clearance from the lung in comparison to WT mice. Additionally, CCR2$^{-/-}$ mice exhibited decreased recruitment of inflammatory monocytes to the lungs in response to both H1N1 alone and H1N1 / MRSA dual infection as compared to WT mice; however, accumulation of CD103+ dendritic cells was significantly enhanced in CCR2$^{-/-}$ mice. Furthermore, CD11c+ DCs from CCR2$^{-/-}$ mice had increased expression of pro-Th17 genes which resulted in increased numbers of IL-17 producing lymphocytes and neutrophils in the lungs following infection. Antagonizing IL-17 partially abrogated the protection seen in CCR2$^{-/-}$ mice. Finally, treatment of infected WT mice with a CCR2 antagonist significantly improved lung bacterial clearance as compared to infected mice treated with saline. Together, these data suggest that neutralization of CCR2 following influenza infection could be efficacious in treating post-influenza secondary bacterial pneumonia.

Materials and Methods

Mouse, virus, and bacteria strains

6- to 8-wk-old C57BL/6 mice were purchased from The Jackson Laboratory (Bar Harbor, ME). The animals were housed in specific pathogen-free conditions within the University of Michigan Animal Care Facility (Ann Arbor, MI) until the day of death or euthanasia. CCR2$^{-/-}$ mice were bred at the University of Michigan and were age and sex matched to WT controls. All animal experiments were performed in accordance with National Institutes of Health policies on the human care and use of laboratory animals and were approved by the Institutional Animal Committee on Use and Care (IACUC) at the University of Michigan.

All experiments used a mouse-adapted influenza A virus (strain A/PR8/34: H1N1 isotype, ATCC) which was inoculated intranasally (i.n.) in a volume of 20 μl containing 100 plaque forming units (pfu).

MRSA strain USA 300 obtained from Network of Antimicrobial Resistance in *Staphylococcus aureus* (NARSA), was grown in Nutrient broth (Difco, Detroit, MI) overnight at 37°C with constant shaking and quantitated by measuring the amount of absorbance at 600 nm compared to a predetermined standard curve. Bacteria were diluted to the desired concentration for oropharyngeal inoculation. Mice were anesthetized with ketamine and xylazine by the intraperitoneal route. For oropharyngeal instillations, 30 μl was deposited by pipet tip to the back of the throat while the tongue was pulled forward. An aliquot of the inoculated MRSA suspension was serially diluted onto nutrient agar plates to determine actual dose of inoculated bacteria.

Antibody purification and administration

We isolated anti-mouse IL-17 antibody from rabbit serum using Pierce Biotechnology Protein A columns and the Thermo Scientific manufacturer's protocol. A Nanodrop 2000 was used to measure concentration by absorbance at 280nm. The specified dose of antibody was diluted with PBS to 100 μL and injected i.p. 6 hours before MRSA inoculation.

Author Manuscript Author Manuscript Author Manuscript Author Manuscript

CCR2 antagonist administration

A small molecule inhibitor of CCR2 identified as PF-04178903 of molecular formula C25 H37 F3 N4 O3 was obtained from Pfizer, Inc. A 50-μg subcutaneous injection of the inhibitor in a volume of 100 μL was administered at the specified time points.

Whole lung homogenization for CFU and cytokine analysis

At designated time-points, mice were euthanized by inhalation of CO_2. The lungs were perfused with 1 mL PBS/5 mM EDTA. Lung tissue was subsequently homogenized in 1 mL PBS with the addition of complete protease inhibitor (Roche, Branford, CT). CXCL1 and CCL2 ELISA assays were performed using Duoset ELISA kits (R&D Systems, Minneapolis, MN) following the manufacturer protocol. Determination of lung bacterial load was measured via serial dilution of whole lung homogenates on nutrient agar plates.

Total lung leukocyte preparation and alveolar epithelial cell isolation

At designated time-points, mice were euthanized by inhalation of CO_2 and lungs were perfused with 3–5 mL PBS / EDTA. Lungs were minced with scissors to a fine slurry in 15 mL lung digestion buffer [DMEM, 10% fetal calf serum, 1 mg / mL collagenase A (Boehringer Mannheim Biochemical) with the addition of 30 μg/ml DNAse (Sigma, St. Louis, MO)]. Lung slurries were enzymatically digested and centrifuged through a 20% Percoll gradient to enrich for leukocytes prior to further analyses. Cell counts, and viability were determined using trypan blue exclusion counting on a hemacytometer.

Alveolar epithelial cells were isolated by dispase digestion of whole lungs after casting the airways in low melt agarose as previously described[27]. Following dispase digestion, hematopoietic cells were negatively selected with CD45 magnetic beads and remaining cells were plated overnight in DMEM +10% FBS to adhere fibroblasts and macrophages. Nonadherent cells containing epithelial cells were then plated on fibronectin coated plates and adhered for 72 h before use.

Bronchoalveolar lavage, neutrophil isolation, and *ex-vivo* neutrophil function assays

Alveolar cells were collected by repeated lavage of the lungs using a total of 20 ml DMEM supplemented with 10% FBS, pen/strep, and L-glutamine via direct cannulation of the trachea with tubing attached to 2 syringes (one to instill media and one to collect media) connected by a 3-way stopcock. For some experiments, neutrophils were isolated following BAL via Ficoll / Histopaque gradient purification. Subsequent ex-vivo determination of bactericidal activity was assayed via addition of MTT as previously described[28].

CD11c cell isolation and isolation of RNA for qRT-PCR

After total lung leukocyte preparation was performed, cells were resuspended up to 10^7 cells in 1mL MACS buffer (Miltenyi Biotec, San Diego, CA), incubated with 100μL of CD11c magnetic microbeads (Miltenyi Biotec, San Diego, CA) and isolated via a quadroMACS magnet in a LS column (Miltenyi Biotec, San Diego, CA). Cells were then counted via a hemacytometer then cytokine measurements were performed.

Author Manuscript Author Manuscript Author Manuscript Author Manuscript

Total RNA was obtained from isolated cells, or whole lung tissue via Trizol extraction following the manufacturer's protocol. RNA concentration was normalized between samples and qRT-PCR was performed on an ABI StepOnePlus real-time thermocycler (Thermo-Fisher, Waltham, MA) using a TaqMan® RNA-to-Ct™ 1-Step Kit (Thermo-Fisher, Waltham, MA) following the manufacturer's protocol. All Primers and probes used in this study are listed in Table1.

Cell marker staining and flow cytometry with tSNE analysis

After total lung leukocyte preparation was performed, nonspecific Fc binding was blocked with a CD16/32 antibody. Subsequently, primary antibodies were added to cell samples and incubated for 30 minutes in the dark at 4°C. Primary antibodies used were anti-CD45, CD11b, CD4, IL-17A, MHCII (I-Ab), CD103, SiglecF (BD Bioscience, San Jose, CA), CD11c, IFNγ (eBioscience San Diego, CA), CD64 (Biolegend, San Diego, CA). For intracellular cytokine staining, cells were first incubated with PMA (10 ng / mL) plus ionomycin (10 μM), with the addition of Golgi-stop reagent (BD Bioscience, San Jose, CA) for 4 h at 37°C. Staining was then performed as above.

T-Distributed Stochastic Nearest-neighbor Embedding (tSNE) was implemented as a plugin in Flowjo v 10.4. Briefly, flow cytometry data for individual samples was concatenated into a single FCS file and a pre-gating strategy was implemented to rid the dataset of cell debris and doublets. Cleaned data was further gated as being Thy1.2+, IL-17+ and the tSNE algorithm was run to separate groups based on the indicated surface markers using the following parameters: perplexity 35, learning rate 1500 for 3000 iterations.

Microscopic imaging and Histopathologic scoring

Lungs were fixed in 4% formaldehyde overnight, and 3-μm paraffin-embedded sections were stained with hematoxylin and eosin (H&E). All images were obtained on an Olympus BX-51 microscope. To assess lung injury, slides were scored in a blinded fashion on a 12 point scale which addressed various aspects of histopathology including alveolar congestion, hemorrhage, presence of neutrophils in the airspaces, and degree of interstitial thickening (0 – 3 points each, based on severity).

For fluorescence imaging of paraffin embedded lung sections, Sections (4 μm) were cut, deparaffinized, and hydrated. Slides were incubated in Target Retrieval Solution (Dako #S1699) for 30 m in a pressure cooker, cooled to RT, and blocked in 5% goat / 5% donkey serum in tris buffered saline with 0.05% Tween (TTBS). Sections were then incubated with anti-pro-SPC (Millipore #AB3786) at 1:500 and anti-T1α (University of Iowa Developmental Studies Hybridoma Bank #8.1.1) at 1:100 overnight at 4°C. After washing in TTBS, sections were incubated with anti-rabbit Cy5 (Jackson #711-605-152) and anti-hamster Cy3 (Jackson #107166–142) antibodies for 1 h at RT, followed by DAPI for 10 m. Images were captures on a Nikon A1 inverted confocal microscope at 10X, serial images were tiled together to form a composite image of the entire lung section.

Author Manuscript Author Manuscript Author Manuscript Author Manuscript

Statistical analyses

Statistical analyses were performed using GraphPad Prism software package (GraphPad Software, La Jolla, CA). Following a normality test, differences between experimental groups were determined using t-tests (for comparing two groups) or one-way ANOVA with a Tukey post-test (for comparing 3 or more groups) if normally distributed. Non-normally distributed data was analyzed by Kruskal-Wallis test and Dunn's multiple comparison post-test. Differences were considered statistically significant when $p < 0.05$. All data are represented as mean +/− SEM. All experiments were repeated, at least, in duplicate with similar results. Pertinent statistical information, i.e. n-values and p-values, are given in individual figure legends.

Results

Mice challenged with H1N1, or H1N1 / MRSA, exhibit elevated levels of CCL2 in lungs.

We utilized a murine model of post-viral bacterial pneumonia. Mice were challenged with 100 pfu of H1N1 i.n. and on day 5 were mock-infected or injected i.t. with 10^7 cfu of MRSA. Prior infection with influenza has previously been shown, by our group and by others, to result in increased bacterial growth as compared to that seen in non-influenza infected WT mice[16, 23]. All samples in this study were collected on day 6 (24 h after MRSA inoculation) unless otherwise specified. We use the shorthand "H1N1/MRSA" to denote sequential infection of H1N1 then MRSA in this model.

To understand the role of CCR2 in this model we wanted to measure expression of CCL2 which serves as a ligand for CCR2. CCL2 has been shown previously to be overexpressed in mouse lungs infected with influenza pneumonia[8]. Our data confirm that cells isolated by bronchoalveolar lavage show massive upregulation of CCL2 mRNA following H1N1 alone, additionally, mice infected with H1N1/MRSA showed a similar increase in CCL2 mRNA following 24 h of bacterial challenge (Figure 1A). Similarly, lung leukocytes show impressive ~80-fold elevations in CCL2 mRNA (Figure 1B). At the protein level, lung homogenates show a 2–3-fold increase in CCL2 protein in mice infected with H1N1, MRSA or H1N1/MRSA (Figure 1C).

Mice deficient in CCR2 have improved survival and bacterial clearance in the lung post H1N1 / MRSA as compared to WT mice.

We next utilized $CCR2^{-/-}$ mice to further address the role of CCR2 during H1N1 / MRSA dual infection or single infection with either H1N1 or MRSA alone. WT and $CCR2^{-/-}$ mice were inoculated with H1N1 and / or MRSA as described above, and lungs were harvested 24 hours post bacterial challenge. Signs of lung injury were apparent following dual infection in WT mice with significant disruption to alveolar epithelial cells as evidenced by fluorescence microscopy for the type 1 alveolar epithelial cell marker T1α, and type II epithelial cell marker surfactant protein C (pro-spc) (Figure 2A). Type II epithelial cells were especially affected in dual infected WT mice and displayed a much less intense staining and lower overall numbers than uninfected (Figure 2A, higher power fields). Patchy type I epithelial cell disruption was also noted (figure 2A yellow arrows). $CCR2^{-/-}$ mice displayed much less type II disruption than WT mice (Figure 2A high power fields), however, a similar level of

Author Manuscript Author Manuscript Author Manuscript Author Manuscript

type I cell disruption was noted (Figure 2A yellow arrows). When examined for other pathologic features (e.g. hemorrhage and leukocyte infiltration) by H&E staining, lungs from CCR2$^{-/-}$ mice exhibited less histopathology overall than WT mice following H1N1 / MRSA dual infection (Figure 2B). Additionally, CCR2$^{-/-}$ mice demonstrated increased survival in comparison to WT mice following this lethal dual infection (Figure 2C). To further address the level of lung injury in dual infected mice we scored H&E stained lung sections following H1N1 / MRSA dual infection based on various criteria of lung injury including: alveolar congestion, hemorrhage, presence of neutrophils in the airspace, and level of interstitial thickening. Consistent with the increased survival, CCR2$^{-/-}$ mice had lower histopathology scores in comparison to WT mice (Figure 2D). Additionally, amounts of BALF-associated albumin (a surrogate measurement for lung protein leakage / lung injury) were also decreased in CCR2$^{-/-}$ mice infected with H1N1 / MRSA in comparison to WT mice (Figure 2E). We next measured both viral and bacterial burdens in WT and CCR2$^{-/-}$ mice following H1N1 / MRSA dual infection. In comparison to WT mice, levels of MRSA cfu were significantly reduced at 24 h post H1N1 / MRSA infection and the same trend was evident at 48h post-infection (Figure 2F). Similarly, in comparison to WT mice, CCR2$^{-/-}$ mice exhibited much lower viral replication indicated by M1 gene expression at both 24 and 48 hpi (6 and 7 days following influenza challenge respectively) (Figure 2G). Interestingly, CCR2$^{-/-}$ mice exhibited minimal changes in comparison to WT mice during single infection with H1N1 or alone. Influenza titers were slightly increased in CCR2$^{-/-}$ mice at 5 dpi (~2-fold Figure S1A) however, this did not reach statistical significance and there was no difference in mortality with both groups reaching euthanasia criteria (percent weight loss) by 8 dpi (Figure S1B). Additionally, as shown in Fig. 3 below, WT and CCR2$^{-/-}$ mice show similar clearance of MRSA infection alone. Taken together these data surprisingly suggest that CCR2$^{-/-}$ mice handle dual infection better than WT mice.

CCR2$^{-/-}$ mice recruit more neutrophils post-infection.

Given that CCR2 generally regulates recruitment of myeloid cells during influenza pneumonia[8,29], we next determined the inflammatory cell composition of the BALF or total lung digestions in uninfected mice, mice infected with H1N1, or mice dual infected with H1N1 / MRSA. Interestingly, the total number of cells recruited to the lung were not significantly different between the groups in WT vs. CCR2$^{-/-}$ mice following single or dual infection, although there was a trend for lower numbers in CCR2$^{-/-}$ mice with H1N1 alone (Figure 3A). In response to H1N1 alone, monocytes and macrophages predominated in the B6 mice, whereas CCR2$^{-/-}$ mice recruited relatively small numbers of monocytes (Figure 3B). In contrast, following H1N1 / MRSA dual infection both WT and CCR2$^{-/-}$ mice recruited predominantly neutrophils, and, CCR2$^{-/-}$ mice exhibited a trend towards increased neutrophil recruitment in comparison to WT mice (Figure 3C). Numbers of lymphocytes remained consistent between all groups (Figure 3D). To assess if neutrophil recruiting chemokines were altered in CCR2$^{-/-}$ mice infected with H1N1, we measured expression of both CXCL1 (KC) and CXCL2 (MIP2) in the lungs by qRT-PCR. Following H1N1 infection alone, CCR2$^{-/-}$ mice displayed a ~3-fold increase in CXCL1 mRNA expression at both 3 and 5 dpi (Figure 3E). A similar increase was noted in the expression of CXCL2 mRNA at 3 dpi (Figure 3F). In agreement with this, amounts of CXCL1 protein, as measured by ELISA, were also elevated in the lungs of H1N1 infected CCR2$^{-/-}$ mice at 3 and 5 dpi (Figure 3G).

Author Manuscript Author Manuscript Author Manuscript Author Manuscript

Given that the CCR2$^{-/-}$ mice expressed more PMN-recruiting chemokines and had higher PMN accumulation post-dual infection, we wanted to verify that PMNs were playing a key role in host defense against MRSA post-H1N1. Thus, WT and CCR2$^{-/-}$ mice were infected with MRSA alone or H1N1/MRSA in the presence or absence of anti-GR1 neutralization to deplete PMNs. Fig 3H demonstrates that anti-GR1 treatment to remove PMNs increases the MRSA cfu in the lung.

CCR2$^{-/-}$ mice produce IL-17 in response to H1N1 infection.

Neutrophils are well documented to be recruited via IL-17[30, 31]. To address if CCR2$^{-/-}$ mice were producing IL-17 following H1N1 infection, we infected WT or CCR2$^{-/-}$ mice i.n. with 100 pfu H1N1. Lungs were harvested at 5 dpi and collagenase digested lung tissue was analyzed via flow cytometry in conjunction with t-SNE dimensional reduction which reduces data for multiple fluorophores into a single two-dimensional plot[32]. Four distinct clusters of IL-17 producing lymphocytes were identified, namely, classic Th17 cells (Thy1.2, CD3+, CD4+), γδ-T cells (Thy1.2+, CD3+, CD4-, γδ-TCR+), and NKT like lymphocytes (Thy1.2+, CD3+, CD4-, NK1.1+) (Figure 4A, histograms detailing surface markers of these populations are shown in Figure S2). In comparison to WT H1N1 infected mice, CCR2$^{-/-}$ mice recruited ~3-fold more IL-17 producing γδ-T cells and ~2.5-fold more Th17 cells (Figure 4B). Numbers of IL-17 producing NKT cells were somewhat higher in CCR2$^{-/-}$ mice, however, this change did not reach statistical significance (Figure 4B). We also detected an interesting population of IL-17, IL-22 co-producing lymphocytes that was increased by ~2-fold in CCR2$^{-/-}$ mice (Figure 4B). Interestingly, numbers of recruited IFNγ-producing Th1 cells, as well as IFNγ-producing CD8+ lymphocytes were not affected with both WT and CCR2$^{-/-}$ mice recruiting equivalent numbers at 5 dpi (Figure 4C, 4D, and 4E).

We further measured expression of IL-17 mRNA in lungs of WT and CCR2$^{-/-}$ mice, following H1N1 single infection, and post-H1N1 / MRSA dual infection. CCR2$^{-/-}$ mice exhibited increased expression of IL-17 at both 3- and 5-days post-influenza infection alone (Figure 4F). Similarly, IL-17 mRNA expression was 4-fold higher in CCR2$^{-/-}$ lungs after H1N1 / MRSA dual infection than in WT lungs (Figure 4G). These data suggest a role for CCR2+ monocytes in modulating or regulating the activation of Th17 cells in response to sequential H1N1 / MRSA infection.

Lung dendritic cell profiles are different in H1N1 or H1N1 / MRSA infected CCR2$^{-/-}$ mice compared to WT mice.

CCR2^{+} monocyte-derived cells have been implicated previously in the immune pathology during influenza infection and CCR2 antagonism offers protection against such pathology[8,33]. Having seen differences in monocyte numbers in lungs post H1N1 infection and sequential infection we wanted to characterize the dendritic cell population accumulating in the lung following H1N1 infection to assess if there were any differences in numbers of dendritic cells accumulated between infected WT and CCR2$^{-/-}$ mice. WT and CCR2$^{-/-}$ mice were infected i.n. with 100 pfu H1N1, 5 dpi, lungs were collagenase digested and flow cytometry was performed to identify the dendritic cell populations present in the lungs. Conventional DCs were identified as CD11c^{+}, MHC II+, CD64-, and SiglecF- (Figure

Author Manuscript Author Manuscript Author Manuscript Author Manuscript

S3). To further identify dendritic cell subsets, cDCs were gated as being either CD103+ or CD11b+ (Figure 5A). CCR2$^{-/-}$ mice exhibited a ~5-fold increase in the number of CD103+ DCs present in the lungs at 5 dpi (Figure 5B). Additionally, CCR2$^{-/-}$ mice displayed a ~2-fold reduction in the number of CD11b DCs (Figure 5C). We next isolated total CD11c+ cells from the lungs of WT or CCR2$^{-/-}$ mice that were uninfected or following H1N1, or H1N1 / MRSA, infection and analyzed them for expression of pro-Th17 transcripts. CD11c + cells isolated from CCR2$^{-/-}$ mice exhibited significant increases in both IL-6 and IL-23 following H1N1 infection in comparison to WT CD11c+ cells (Figure 5D and 5E). No change in IL-1β transcript was detected in CCR2$^{-/-}$ mice in comparison to WT; however, both groups showed elevated IL-1β in comparison to uninfected control groups (Figure 5F). Similar trends in IL-6 and IL-23 expression were also noted following H1N1 / MRSA dual infection (Figure 5G and 5H). Additionally, CD11c+ cells isolated from dual infected CCR2$^{-/-}$ mice displayed a ~2-fold reduction in IL-27 transcript expression (Figure 5I). These data strongly suggest that resident CD103+ DCs in CCR2$^{-/-}$ mice are responsible for skewing effector T cell responses towards Th17. Additionally, the cytokine milieu is likely to influence IL-17 production by other lymphocyte subsets as well.

Influenza induces expression of IL-17 receptor on lung epithelial cells to promote CXCL1 induction.

Given that CCR2$^{-/-}$ mice express more IL-17, we tested the influence of influenza on expression of IL-17R on lung epithelial cells. Type II epithelial cells were isolated from both WT and CCR2$^{-/-}$ mice and infected *in vitro* with H1N1, at a MOI of 0.01 for 48 h and expression of IL-17 receptor was subsequently analyzed by qRT-PCR. Interestingly, H1N1 infection upregulated expression of IL-17R in epithelial cells from both genotypes, but there was no differential expression between WT and CCR2$^{-/-}$ mice (Fig. 6A). When expression of CXCL1 was assessed in epithelial cell cultures infected with H1N1 in the presence and absence of IL-17, we found that the addition of either IL-17 or H1N1 alone was sufficient to increase CXCL1 expression by AECs, however, an additive increase in CXCL1 expression was observed when AECs were administered both IL-17 and H1N1 simultaneously (Fig. 6B).

Antagonism of CCR2 in WT mice improves bacterial clearance and elicits a pro-Th17 response.

To determine if antagonism of CCR2 held therapeutic potential in our model of post-viral bacterial pneumonia, we treated WT mice with a small molecule inhibitor of CCR2, PF-04178903, twice daily for five days from day 0 through day 5 post-H1N1 and prior to MRSA infection. On day 6, lung homogenate cultures isolated from WT mice treated with PF-04178903 compared to untreated WT mice demonstrated 10-fold lower bacterial cfu of MRSA, respectively (Figure 7A). Consistent with the CCR2$^{-/-}$ mice, PF-04178903 treated mice had a marked increase in segmented neutrophil infiltration to the lung following MRSA infection (Figure 7B). In conjunction with lower bacterial counts in lungs, treated WT mice had increased expression of the pro-Th17 genes IL-1β and IL-6 (Figure 7C). Additionally, IL-17α, and the neutrophil attracting chemokines CXCL1 and CXCL2 were also increased in CCR2 antagonist treated mice (Figure 7C).

Author Manuscript Author Manuscript Author Manuscript Author Manuscript

To further implicate IL-17 as a mechanism of protection in CCR2$^{-/-}$ mice, we treated CCR2$^{-/-}$ mice with a neutralizing IL-17 antibody in comparison to isotype antibody. Anti-IL-17 antibody was purified from rabbit serum and injected intraperitoneally 6 hours prior to MRSA infection in our model. Unfortunately, we only obtained enough antisera to treat 2 mice per group with 200μg anti-IL-17 or control antibody (Figure S4); however, there was a trend towards IL-17 neutralization impairing bacterial clearance in CCR2$^{-/-}$ mice (p=0.01).

Discussion

The results of earlier studies have shown specific influenza A virus subtypes modulate innate immune responses including antigen presenting cell populations, pattern-recognition receptor activation, recruitment of cells via chemotaxis, and cytokine expression[34–37]. These mechanisms not only worsen morbidity and mortality from immunopathology, but also increase susceptibility to secondary bacterial infection after influenza pneumonia. In our study, expression of CCL2 was dramatically increased following H1N1 / MRSA (Figure 1) in wild-type mice and this was associated with recruitment of monocytes and neutrophils (Figure 3). Interestingly however, CCR2$^{-/-}$ mice were better protected from secondary bacterial pneumonia following influenza and displayed much lower levels of epithelial disruption and lung pathology (Figure 2A and 2D) as well as increased survival and greatly augmented bacterial clearance as compared to WT mice (Figure 2C and 2F). Innate immune cells are responsible for clearance of MRSA in the first 24 h post-infection; yet, wild-type mice ineffectively clear bacteria in the first 24 hours of infection post-H1N1. Further, this defect correlates with increased levels of CCL2 suggesting that recruitment of CCR2^{+} monocyte-derived DCs and exudative macrophages not only contribute to immunopathology and mortality but are surprisingly associated with higher bacterial burden in lung.

CCR2^{+} monocytes have previously been implicated in the pathogenesis of pneumonia associated with single influenza infection and blockade of CCR2 signaling using a CCR2 antagonist significantly increased survival against influenza single-challenge[33]. More recently, influenza A was found to drive robust CCL2 (MCP-1) expression in juvenile mice and this expression was correlated with increased lethality of influenza in comparison to aged mice[9]. Our results suggest that CCR2 signaling is similarly pathogenic in the setting of H1N1 / MRSA dual infection.

Here we present data that loss of CCR2 results in increased neutrophil accumulation in response to MRSA following H1N1 infection (Figure 3C). Paradoxically, CCR2 has been shown to be expressed by, at least, some subsets of neutrophils[38, 39]. However, the neutrophil attracting chemokines CXCL1, and CXCL2 (KC and MIP-2) were similarly up-regulated following H1N1 / MRSA infection in CCR2$^{-/-}$ mice (Figure 3E, 3F, and 3G) and thus neutrophil recruitment was probably mediated through the more canonical CXCL1 / 2 - CXCR2 axis. Interestingly neutrophils, not inflammatory monocytes, have been shown to be important for the clearance of S. *aureus*; however, CCR2^{+} monocytes are important for wound resolution following bacterial clearance[40]. Furthermore, clearance of S. *pneumoniae*, another common cause of post-influenza secondary bacterial pneumonia, was also shown to rely in part on neutrophil mediated mechanisms[41]. In support of this, we depleted neutrophils in CCR2$^{-/-}$ mice by i.p. injection of αGR1 neutralizing antibody and observed a

Author Manuscript Author Manuscript Author Manuscript Author Manuscript

~100-fold increase in bacterial burden in treated mice indicating that neutrophils are the major clearance mechanism of MRSA following H1N1 infection (Figure 3H). Thus, it is possible that one reason the $CCR2^{-/-}$ mice do better is because their lungs essentially only have neutrophils present to fight the bacterial infection whereas the wild-type lungs would have a mixture of both monocytes and neutrophils and the increased cfu in these mice may reflect the poorer functionality of the monocytes relative to the neutrophils. We compared lung derived (following LPS stimulation) neutrophils isolated from $CCR2^{-/-}$ mice to WT neutrophils in both their ability to phagocytize and to kill MRSA bacterium ex-vivo. No difference in phagocytic capacity was noted between $CCR2^{-/-}$ and WT neutrophils; however, there was a small but statistically significant increase in the ability of $CCR2^{-/-}$ neutrophils to kill MRSA (Figure S5). It should be noted that $CCR2^{+}$ monocytes are important for the clearance of, at least, some bacterial infections. Specifically, depletion of $CCR2^{+}$ cells resulted in increased growth and increased lethality, to certain strains, in a mouse model of pulmonary *Klebsiella pneumoniae* infection[11, 13]. Furthermore, at least one study found that lung specific overexpression of CCL2 enhanced immune responses towards *S. pneumoniae*; however, CCR2 neutralization had no effect on bacterial killing in an H1N1 / S. *pneumoniae* model of secondary bacterial pneumonia[14, 33]. Thus, while our data indicate that loss of CCR2 signaling enhances neutrophil recruitment, neutrophil associated bacterial killing, and confers protection from secondary MRSA-associated pneumonia, further studies must necessarily examine these effects with regards to other bacterial infections.

In the influenza immunity field, there is ample evidence implicating the viral infection in altering the cytokine profile “bridge” that links the innate and adaptive immune responses. Several reports have shown increased expression of IL-12, IFN-γ, IL-2, and TNF-α, which are all markers of Th1 polarization that are present after influenza pneumonia[12, 36, 42–44]. Morbidity and mortality have been primarily attributed to immunopathology in the context of a Th1 response[8]. In bacterial superinfection with S. *aureus*, the type 1 response and associated immunopathology is amplified. However, beneficial Th17 immunity is suppressed in these mouse models. Robinson *et al*. rescued protective Th17 pathway activation, increased survival, decreased bacterial burden, and reduced lung injury with administration of exogenous IL-1β, an activator of Th17 differentiation and thus production of Th17 associated cytokines like IL-17 and IL-22[22]. Separately, Kudva *et al*. demonstrated downstream effectors of the Th17 pathway such as antimicrobial peptides (AMPs) are essential to defense against *S. aureus* pneumonia after influenza challenge[16]. In both studies, other markers of Th17 including IL-17 and IL-23 were present. We previously published that loss of CCR2 signaling increased Th17 differentiation and IL-17 production in response to γ-herpesviruses[26]. In agreement with this, $CCR2^{-/-}$ mice recruited increased numbers of IL-17 secreting lymphocytes in response to H1N1 infection (Figure 4A and 4B) and had increased expression of IL-17 in the lungs following either H1N1 or H1N1 / MRSA infection (Figure 4F and 4G). Interestingly, multiple subsets of IL-17 secreting cells were increased in $CCR2^{-/-}$ mice, including, classic Th17 cells, and the more innate-like γδ- T cells and NK1.1+ NKT cells (Figure 4A). Both γδ-Tcells and NKT cells are rapidly recruited to the lung following S. *aureus* infection and play a role in host defense through secretion of IL-17[45, 46]. We also detected a subpopulation of IL-17 / IL-22 co-producing

Author Manuscript Author Manuscript Author Manuscript Author Manuscript

cells that was markedly upregulated in CCR2$^{-/-}$ mice following H1N1 / MRSA infection. IL-22 has been implicated as a negative regulator of S. *aureus* colonization[47]. Further, induction of IL-17 and IL-22 by IL-1β was previously shown to be protective in an H1N1 / MRSA model via up-regulation of the antimicrobial peptide RegIIIβ[22]. Thus, it is likely that the cytokine profile of the DCs are impacting development of both classic Th17 cells as well as IL-17-expressing innate lymphocytes. Importantly, numbers of interferon-γ secreting Th1 and CD8+ cells were not altered in CCR2$^{-/-}$ mice indicating that anti-viral responses were intact (Figure 4C and 4D). Interestingly, there is some evidence that both IL-17 and IFNγ are necessary for effective clearance of S. *aureus* and IFNγRI$^{-/-}$ / IL-17Rα$^{-/-}$ dual knockout mice have defects in neutrophil function that render them more susceptible to S. *aureus* infection[48]. Thus, genetic ablation of CCR2 appears to augment recruitment of IL-17 secreting lymphocytes while maintaining production of IFNγ resulting in an increased capacity to clear S. *aureus* bacteria.

To identify the key leukocytes responsible for the protective CCR2$^{-/-}$ phenotype, we performed flow cytometry on cells isolated from Percoll gradients of enzymatically digested lung. In the context of H1N1 infection, CCR2$^{-/-}$ mice accumulated an increased number of CD103^{+} DCs (Figure 5B) as well as reduced numbers of CD11b+ DCs than WT mice (Figure 5C) in the lung. Intestinal CD103+ DCs have previously been shown to be major producers of IL-23 in response to bacteria[49]. Moreover lung CD103+ DCs have been shown to play a critical role in induction of Influenza virus-specific CD8^{+} T cells[50]. In support of our observation that altered DC subsets which accumulate in the lungs CCR2$^{-/-}$ mice can drive Th17 differentiation and IL-17 production, we report that CD11c+ cells isolated from the lungs of CCR2$^{-/-}$ mice infected with either H1N1 alone, or H1N1 / MRSA exhibited a pro-Th17 cytokine profile with increased expression of IL-6 and IL-23 in comparison to infected WT mice (Figure 5D, 5E, 5G, and 5H) as well as elevated levels of IL-1β in comparison to uninfected mice (Figure 5F). We also report that IL-27 is expressed at a lower level in the lungs of CCR2$^{-/-}$ mice compared to WT mice (Figure 5I). Expression of IL-27 has previously been linked to increased susceptibility to secondary bacterial pneumonia following H1N1 infection[51]. IL-27 has also been implicated as a suppressor of Th17 differentiation and there is evidence to suggest that CD11b+ DCs are responsible for IL-27 secretion[52, 53]. Thus, we hypothesize that the alterations in the ratios of CD103+ to CD11b+ DC subsets are responsible for increased expression of IL-6 and IL-23 along with abrogated expression of IL-27 in the absence of CCR2. CD103+ DCs are likely unaffected by loss of CCR2 as they are the resident DC population in the lung whereas CD11b+ DCs utilize CCR2 for migration to the lung[54, 55]. Interestingly, infection with H1N1 alone increased expression of the IL-17 receptor on AECs and co-incubation of AECs with both H1N1 and IL-17 greatly increased CXCL1 expression (Figure 6A and 6B). However, the DC subsets that are recruited in response to H1N1 in WT mice are insufficient to drive robust Th17 differentiation and may in fact actively suppress it, acting as a detriment to bacterial clearance.

To implicate IL-17 as the mechanism for improved bacterial clearance in CCR2$^{-/-}$ lungs compared to WT, we performed IL-17 neutralization studies. Inhibition of IL-17 in CCR2$^{-/-}$ mice using i.p. administration of purified rabbit-anti-mouse IL-17α antibody prior to MRSA infection increased bacterial burden in CCR2$^{-/-}$ lungs relative to lungs of CCR2$^{-/-}$ mice

Author Manuscript Author Manuscript Author Manuscript Author Manuscript

treated with isotype control antibody (Figure S4). We further validated this finding by inhibiting CCR2 in WT mice using a small molecule compound, PF-04178903, injected twice daily for 5 days starting on day of H1N1 inoculation. This compound has been used previously by Lin et al to antagonize CCR2 in a murine model of influenza pneumonia[33]. In their study, CCR2 inhibition reduced immunopathology in an influenza pneumonia model. We show that antagonism of CCR2 in a post-influenza pneumonia model improves MRSA clearance associated with increased expression of IL-17 (Figure 7).

Our conclusion is that CCR2-dependent recruitment of DCs/macrophages during postinfluenza MRSA pneumonia contributes to inhibition of Th17 and innate IL-17-expressing cells, and this process has profound negative effects on bacterial clearance in the lung. The data presented in this manuscript provide further evidence that the Th17 pathway is crucial in opposing the immunomodulatory effects of influenza that confer susceptibility to bacterial superinfection, lung injury, and death. We believe that antagonizing CCR2 would provide a potential therapeutic target and significantly decrease mortality and morbidity associated with influenza and post influenza bacterial pneumonia.

Supplementary Material

Refer to Web version on PubMed Central for supplementary material.

Acknowledgements

This work was supported by NIH grants HL127805, HL115618 and AI117229 to BBM.

Grant support: HL119682, AI117229 (BBM)

References

1. Rice T, Rubinson L, Uyeki T. Critical Illness from 2009 Pandemic Influenza A (H1N1) Virus and Bacterial Co-Infection in the United States. Critical care… 2012; 40: 1487–1498.
2. Peiris JSM, Hui KPY, Yen H-L. Host response to influenza virus: protection versus immunopathology. Current opinion in immunology 2010; 22: 475–481. [PubMed: 20594815]
3. Smith AM, McCullers JA. Secondary bacterial infections in influenza virus infection pathogenesis. Curr Top Microbiol Immunol 2014; 385: 327–356. [PubMed: 25027822]
4. Murray RJ, Robinson JO, White JN, Hughes F, Coombs GW, Pearson JC et al. Community-acquired pneumonia due to pandemic A(H1N1)2009 influenzavirus and methicillin resistant Staphylococcus aureus co-infection. PLoS One 2010; 5(1): e8705. [PubMed: 20090931]
5. McGill J, Heusel JW, Legge KL. Innate immune control and regulation of influenza virus infections. Journal of leukocyte biology 2009; 86: 803–812. [PubMed: 19643736]
6. Gouwy M, Struyf S, Leutenez L, Pörtner N, Sozzani S, Van Damme J. Chemokines and other GPCR ligands synergize in receptor-mediated migration of monocyte-derived immature and mature dendritic cells. Immunobiology 2014; 219: 218–229. [PubMed: 24268109]
7. van Helden MJG, Zaiss DMW, Sijts AJaM. CCR2 defines a distinct population of NK cells and mediates their migration during influenza virus infection in mice. PloS one 2012; 7: e52027. [PubMed: 23272202]
8. Lin KL, Suzuki Y, Nakano H, Ramsburg E, Gunn MD. CCR2+ monocyte-derived dendritic cells and exudate macrophages produce influenza-induced pulmonary immune pathology and mortality. Journal of immunology (Baltimore, Md: 1950) 2008; 180: 2562–2572.
9. Coates BM, Staricha KL, Koch CM, Cheng Y, Shumaker DK, Budinger GRS et al. Inflammatory Monocytes Drive Influenza A Virus-Mediated Lung Injury in Juvenile Mice. J Immunol 2018.

Author Manuscript Author Manuscript Author Manuscript Author Manuscript

10. Kroetz DN, Allen RM, Schaller MA, Cavallaro C, Ito T, Kunkel SL. Type I Interferon Induced Epigenetic Regulation of Macrophages Suppresses Innate and Adaptive Immunity in Acute Respiratory Viral Infection. PLoS Pathog 2015; 11(12): e1005338. [PubMed: 26709698]
11. Xiong H, Carter RA, Leiner IM, Tang YW, Chen L, Kreiswirth BN et al. Distinct Contributions of Neutrophils and CCR2+ Monocytes to Pulmonary Clearance of Different Klebsiella pneumoniae Strains. Infect Immun 2015; 83(9): 3418–3427. [PubMed: 26056382]
12. Pietras EM, Miller LS, Johnson CT, O'Connell RM, Dempsey PW, Cheng G. A MyD88-dependent IFNγR-CCR2 signaling circuit is required for mobilization of monocytes and host defense against systemic bacterial challenge. Cell research 2011; 21: 1068–1079. [PubMed: 21467996]
13. Xiong H, Keith JW, Samilo DW, Carter RA, Leiner IM, Pamer EG. Innate Lymphocyte/Ly6C(hi) Monocyte Crosstalk Promotes Klebsiella Pneumoniae Clearance. Cell 2016; 165(3): 679–689. [PubMed: 27040495]
14. Winter C, Taut K, Srivastava M, Langer F, Mack M, Briles DE et al. Lung-specific overexpression of CC chemokine ligand (CCL) 2 enhances the host defense to Streptococcus pneumoniae infection in mice: role of the CCL2-CCR2 axis. J Immunol 2007; 178(9): 5828–5838. [PubMed: 17442967]
15. Frank KM, Zhou T, Moreno-Vinasco L, Hollett B, Garcia JGN, Bubeck Wardenburg J. Host response signature to Staphylococcus aureus alpha-hemolysin implicates pulmonary Th17 response. Infection and immunity 2012; 80: 3161–3169. [PubMed: 22733574]
16. Kudva A, Scheller EV, Robinson KM, Crowe CR, Choi SM, Slight SR et al. Influenza A inhibits Th17-mediated host defense against bacterial pneumonia in mice. Journal of immunology (Baltimore, Md: 1950) 2011; 186: 1666–1674.
17. Cao J, Wang D, Xu F, Gong Y, Wang H, Song Z et al. Activation of IL-27 signalling promotes development of postinfluenza pneumococcal pneumonia. EMBO molecular medicine 2014; 6: 120–140. [PubMed: 24408967]
18. Cho JS, Pietras EM, Garcia NC, Ramos RI, Farzam DM, Monroe HR et al. IL-17 is essential for host defense against cutaneous Staphylococcus aureus infection in mice. J Clin Invest 2010; 120(5): 1762–1773. [PubMed: 20364087]
19. Bosmann M, Grailer JJ, Russkamp NF, Ruemmler R, Zetoune FS, Sarma JV et al. CD11c+ alveolar macrophages are a source of IL-23 during lipopolysaccharide-induced acute lung injury. Shock (Augusta, Ga) 2013; 39: 447–452.
20. Iwakura Y, Ishigame H. The IL-23/IL-17 axis in inflammation. The Journal of clinical investigation 2006; 116: 1218–1222. [PubMed: 16670765]
21. Trinchieri G Interleukin-12 and the regulation of innate resistance and adaptive immunity. Nature reviews Immunology 2003; 3: 133–146.
22. Robinson KM, Choi SM, McHugh KJ, Mandalapu S, Enelow RI, Kolls JK et al. Influenza A exacerbates Staphylococcus aureus pneumonia by attenuating IL-1β production in mice. Journal of immunology (Baltimore, Md: 1950) 2013; 191: 5153–5159.
23. Podsiad A, Standiford TJ, Ballinger MN, Eakin R, Park P, Kunkel SL et al. MicroRNA-155 regulates host immune response to postviral bacterial pneumonia via IL-23/IL-17 pathway. Am J Physiol Lung Cell Mol Physiol 2016; 310(5): L465–475. [PubMed: 26589478]
24. Robinson KM, McHugh KJ, Mandalapu S, Clay ME, Lee B, Scheller EV et al. Influenza A virus exacerbates Staphylococcus aureus pneumonia in mice by attenuating antimicrobial peptide production. The Journal of infectious diseases 2014; 209: 865–875. [PubMed: 24072844]
25. Sun K, Metzger DW. Influenza Infection Suppresses NADPH Oxidase-Dependent Phagocytic Bacterial Clearance and Enhances Susceptibility to Secondary Methicillin-Resistant Staphylococcus aureus Infection. Journal of immunology (Baltimore, Md: 1950) 2014; 192: 3301–3307.
26. Gurczynski SJ, Procario MC, O'Dwyer DN, Wilke CA, Moore BB. Loss of CCR2 signaling alters leukocyte recruitment and exacerbates gamma-herpesvirus-induced pneumonitis and fibrosis following bone marrow transplantation. Am J Physiol Lung Cell Mol Physiol 2016; 311(3): L611–627. [PubMed: 27448666]

Author Manuscript Author Manuscript Author Manuscript Author Manuscript

27. Bauman KA, Wettlaufer SH, Okunishi K, Vannella KM, Stoolman JS, Huang SK et al. The antifibrotic effects of plasminogen activation occur via prostaglandin E2 synthesis in humans and mice. J Clin Invest 2010; 120(6): 1950–1960. [PubMed: 20501949]
28. Ballinger MN, Paine R, 3rd, Serezani CH, Aronoff DM, Choi ES, Standiford TJ et al. Role of granulocyte macrophage colony-stimulating factor during gram-negative lung infection with Pseudomonas aeruginosa. Am J Respir Cell Mol Biol 2006; 34(6): 766–774. [PubMed: 16474098]
29. Dawson TC, Beck Ma, Kuziel Wa, Henderson F, Maeda N. Contrasting effects of CCR5 and CCR2 deficiency in the pulmonary inflammatory response to influenza A virus. The American journal of pathology 2000; 156: 1951–1959. [PubMed: 10854218]
30. Ye P, Rodriguez FH, Kanaly S, Stocking KL, Schurr J, Schwarzenberger P et al. Requirement of interleukin 17 receptor signaling for lung CXC chemokine and granulocyte colony-stimulating factor expression, neutrophil recruitment, and host defense. J Exp Med 2001; 194(4): 519–527. [PubMed: 11514607]
31. Chen K, Eddens T, Trevejo-Nunez G, Way EE, Elsegeiny W, Ricks DM et al. IL-17 Receptor Signaling in the Lung Epithelium Is Required for Mucosal Chemokine Gradients and Pulmonary Host Defense against K. pneumoniae. Cell Host Microbe 2016; 20(5): 596–605. [PubMed: 27923703]
32. Maaten Lvd, Hinton G. Visualzing Data using t-SNE. Journal of machine Learning Research 2008; 9: 2579–2605.
33. Lin KL, Sweeney S, Kang BD, Ramsburg E, Gunn MD. CCR2-antagonist prophylaxis reduces pulmonary immune pathology and markedly improves survival during influenza infection. Journal of immunology (Baltimore, Md: 1950) 2011; 186: 508–515.
34. Beauchamp NM, Yammani RD, Alexander-Miller Ma. CD8 marks a subpopulation of lung-derived dendritic cells with differential responsiveness to viral infection and toll-like receptor stimulation. Journal of virology 2012; 86: 10640–10650. [PubMed: 22811544]
35. Damjanovic D, Divangahi M, Kugathasan K, Small CL, Zganiacz A, Brown EG et al. Negative regulation of lung inflammation and immunopathology by TNF-alpha during acute influenza infection. Am J Pathol 2011; 179(6): 2963–2976. [PubMed: 22001698]
36. Sun K, Metzger DW. Inhibition of pulmonary antibacterial defense by interferon-gamma during recovery from influenza infection. Nature medicine 2008; 14: 558–564.
37. Huang Y, Zhu W, Zeng X, Li S, Li X, Lu C. Innate and adaptive immune responses in patients with pandemic influenza A(H1N1)pdm09. Archives of virology 2013; 158: 2267–2272. [PubMed: 23728719]
38. Fujimura N, Xu B, Dalman J, Deng H, Aoyama K, Dalman RL. CCR2 inhibition sequesters multiple subsets of leukocytes in the bone marrow. Sci Rep 2015; 5: 11664. [PubMed: 26206182]
39. Souto FO, Alves-Filho JC, Turato WM, Auxiliadora-Martins M, Basile-Filho A, Cunha FQ. Essential role of CCR2 in neutrophil tissue infiltration and multiple organ dysfunction in sepsis. Am J Respir Crit Care Med 2011; 183(2): 234–242. [PubMed: 20732989]
40. Feuerstein R, Seidl M, Prinz M, Henneke P. MyD88 in macrophages is critical for abscess resolution in staphylococcal skin infection. J Immunol 2015; 194(6): 2735–2745. [PubMed: 25681348]
41. Deniset JF, Surewaard BG, Lee WY, Kubes P. Splenic Ly6Ghigh mature and Ly6Gint immature neutrophils contribute to eradication of S. pneumoniae. J Exp Med 2017; 214(5): 1333–1350. [PubMed: 28424248]
42. Moltedo B, López CB, Pazos M, Becker MI, Hermesh T, Moran TM. Cutting edge: stealth influenza virus replication precedes the initiation of adaptive immunity. Journal of immunology (Baltimore, Md: 1950) 2009; 183: 3569–3573.
43. Hagau N, Slavcovici A, Gonganau DN, Oltean S, Dirzu DS, Brezoszki ES et al. Clinical aspects and cytokine response in severe H1N1 influenza A virus infection. Critical care (London, England) 2010; 14: R203.
44. Bermejo-Martin JF, Ortiz de Lejarazu R, Pumarola T, Rello J, Almansa R, Ramírez P et al. Th1 and Th17 hypercytokinemia as early host response signature in severe pandemic influenza. Critical care (London, England) 2009; 13: R201.

Author Manuscript Author Manuscript Author Manuscript Author Manuscript

45. Cheng P, Liu T, Zhou WY, Zhuang Y, Peng LS, Zhang JY et al. Role of gamma-delta T cells in host response against Staphylococcus aureus-induced pneumonia. BMC Immunol 2012; 13: 38. [PubMed: 22776294]

46. Small CL, McCormick S, Gill N, Kugathasan K, Santosuosso M, Donaldson N et al. NK cells play a critical protective role in host defense against acute extracellular Staphylococcus aureus bacterial infection in the lung. J Immunol 2008; 180(8): 5558–5568. [PubMed: 18390740]

47. Mulcahy ME, Leech JM, Renauld JC, Mills KH, McLoughlin RM. Interleukin-22 regulates antimicrobial peptide expression and keratinocyte differentiation to control Staphylococcus aureus colonization of the nasal mucosa. Mucosal Immunol 2016; 9(6): 1429–1441. [PubMed: 27007677]

48. Barin JG, Talor MV, Schaub JA, Diny NL, Hou X, Hoyer M et al. Collaborative Interferon-gamma and Interleukin-17 Signaling Protects the Oral Mucosa from Staphylococcus aureus. Am J Pathol 2016; 186(9): 2337–2352. [PubMed: 27470712]

49. Kinnebrew Ma, Buffie CG, Diehl GE, Zenewicz La, Leiner I, Hohl TM et al. Interleukin 23 Production by Intestinal CD103 +CD11b + Dendritic Cells in Response to Bacterial Flagellin Enhances Mucosal Innate Immune Defense. Immunity 2012; 36: 276–287. [PubMed: 22306017]

50. Helft J, Manicassamy B, Guermonprez P, Hashimoto D, Silvin A, Agudo J et al. Cross-presenting CD103+ dendritic cells are protected from influenza virus infection. The Journal of… 2012; 122: 4037–4047.

51. Robinson KM, Lee B, Scheller EV, Mandalapu S, Enelow RI, Kolls JK et al. The role of IL-27 in susceptibility to post-influenza Staphylococcus aureus pneumonia. Respir Res 2015; 16: 10. [PubMed: 25651926]

52. Wang L, Li Z, Ciric B, Safavi F, Zhang GX, Rostami A. Selective depletion of CD11c(+) CD11b(+) dendritic cells partially abrogates tolerogenic effects of intravenous MOG in murine EAE. Eur J Immunol 2016; 46(10): 2454–2466. [PubMed: 27338697]

53. Stumhofer JS, Laurence A, Wilson EH, Huang E, Tato CM, Johnson LM et al. Interleukin 27 negatively regulates the development of interleukin 17-producing T helper cells during chronic inflammation of the central nervous system. Nat Immunol 2006; 7(9): 937–945. [PubMed: 16906166]

54. Osterholzer JJ, Chen G-H, Olszewski Ma, Curtis JL, Huffnagle GB, Toews GB. Accumulation of CD11b+ lung dendritic cells in response to fungal infection results from the CCR2-mediated recruitment and differentiation of Ly-6Chigh monocytes. Journal of immunology (Baltimore, Md : 1950) 2009; 183: 8044–8053.

55. Plantinga M, Guilliams M, Vanheerswynghels M, Deswarte K, Branco-Madeira F, Toussaint W et al. Conventional and monocyte-derived CD11b(+) dendritic cells initiate and maintain T helper 2 cell-mediated immunity to house dust mite allergen. Immunity 2013; 38(2): 322–335. [PubMed: 23352232]

Author Manuscript Author Manuscript Author Manuscript Author Manuscript

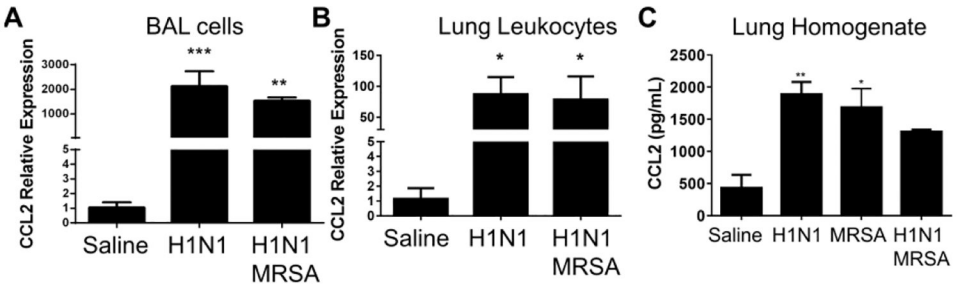

Figure 1. Expression of CCL2 (MCP-1) in the lung is increased following H1N1 infection or H1N1 / MRSA dual infection.

(A) Bronchoalveolar lavage (BAL) was performed on uninfected, H1N1 or H1N1 / MRSA dual infected WT mice (6 days after H1N1 infection, 24 hours following MRSA infection). CCL2 expression was measured via qRT-PCR from isolated BAL cells. **(B)** Leukocytes were harvested from collagenase digested lung tissue 24 hours after MRSA infection (6 days after H1N1 infection). CCL2 expression was measured via qRT-PCR. **(C)** Whole lung homogenates were prepared 24 hours after MRSA infection (6 days following H1N1 infection). CCL2 was quantified by ELISA. Statistical significance was calculated by Kruskal Wallis non-parametric test, * $p < 0.05$, ** $p < 0.01$ versus uninfected. n = 3 mice per group.

Author Manuscript Author Manuscript Author Manuscript Author Manuscript

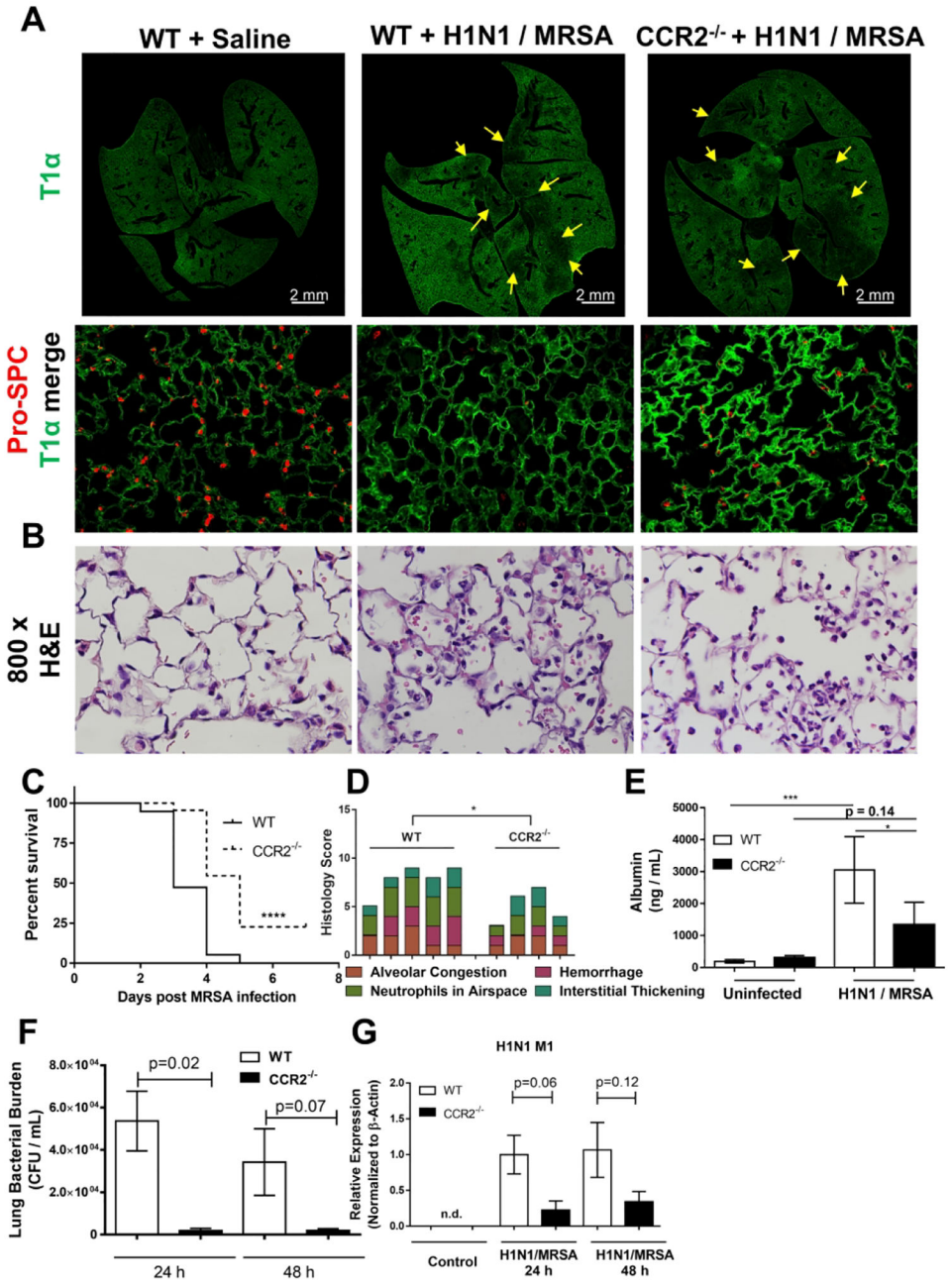

Figure 2. Loss of CCR2 signaling facilitates bacterial clearance and increases survival in H1N1 / MRSA dual infected mice.

(A and B) WT or CCR2$^{-/-}$ mice were infected for 5d with H1N1 and subsequently infected with MRSA for 24 h. Formalin fixed lung sections were prepared and stained with pro-SPC and T1α as markers for type 2 and type1 alveolar epithelial cells respectively **(A)** or H&E **(B)** (representative images of n = 4 mice per group). **(C)** Survival curves of WT and CCR2$^{-/-}$ mice following H1N1 / MRSA (n = 19 mice per group). **(D)** Histology scoring of either WT or CCR2$^{-/-}$ mouse infected with H1N1 / MRSA (n = 4 – 5 mice per group). **(E)** BAL was performed on uninfected or H1N1 / MRSA infected mouse groups and albumin was quantified from BALF by ELISA (n = 3 – 5 mice per group). **(F)** Lung CFU from WT

Author Manuscript Author Manuscript Author Manuscript Author Manuscript

mice and CCR2$^{-/-}$ mice following sequential infection with H1N1 and MRSA. **(G)** Expression of the H1N1 *M1* gene as measured by qRT-PCR (n = 3 mice per group). Statistical significance calculated using ANOVA, * = $p < 0.05$, ** = $p < 0.01$, **** = $p < 0.0001$.

Author Manuscript Author Manuscript Author Manuscript Author Manuscript

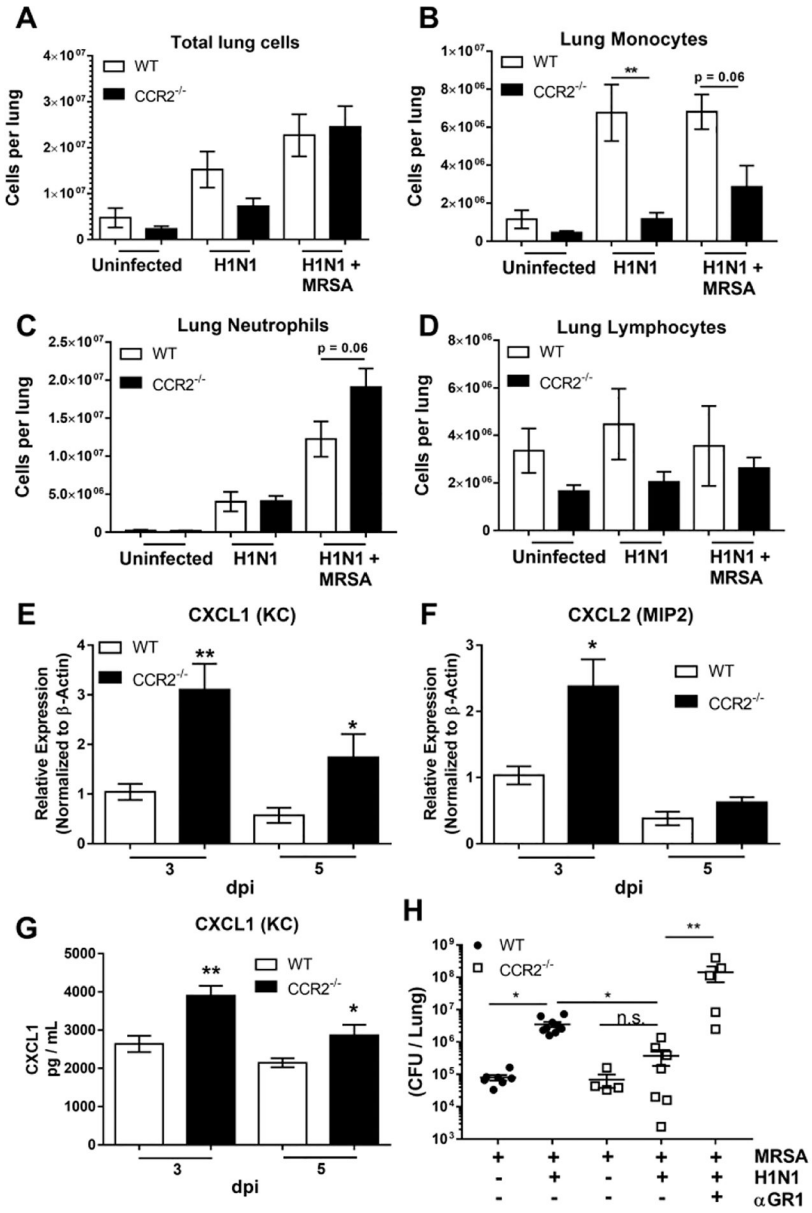

Figure 3. CCR2$^{-/-}$ mice recruit neutrophils instead of monocytes following H1N1 / MRSA infection.

(A) Total leukocytes obtained from enzymatically digested lung. **(B, C, and D)** Total leukocytes from lung homogenates were prepared for cytospin and counted manually following differential staining. **(E and F)** WT or CCR2$^{-/-}$ mice were infected for 3 or 5 days with H1N1. Total RNA was extracted and analyzed for expression of the indicated transcript. **(G)** Lung homogenates were prepared from WT or CCR2$^{-/-}$ mice infected for 3 or 5 days with H1N1 alone and the amount of CXCL1 protein was determined by ELISA. **(H)** WT or CCR2$^{-/-}$ mice were infected with the indicated pathogen and treated with αGR1 antibody to deplete neutrophils, lung bacterial burden was determined by serial dilution of lung homogenate. Statistical significance was determined by ANOVA, or Kruskal Wallis non-parametric test in panel H. * $p < 0.05$, ** $p < 0.01$ (n = 4 – 9 mice per group).

Author Manuscript
Author Manuscript
Author Manuscript
Author Manuscript

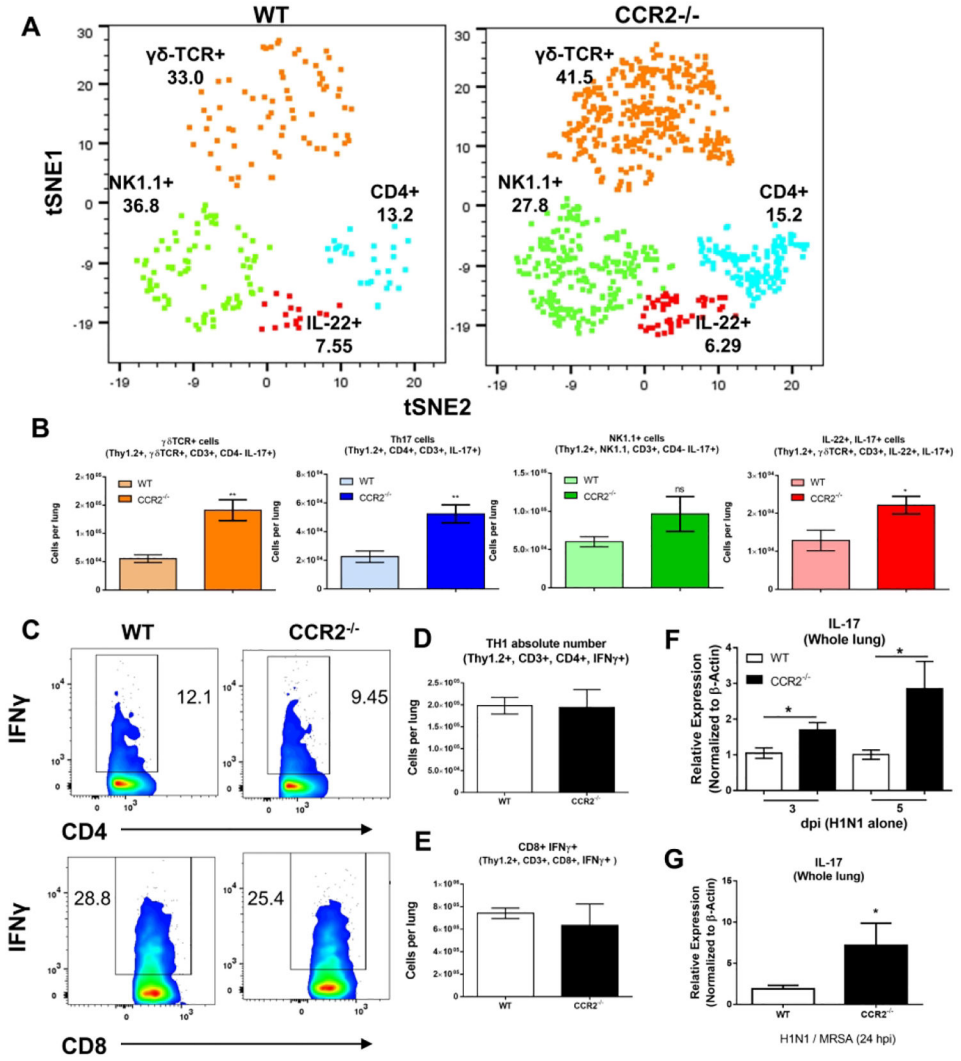

Figure 4. Abrogation of CCR2 signaling results in increased infiltration of IL-17 producing lymphocytes and increased expression of IL-17 in the lungs following H1N1 or H1N1 / MrSa dual infection.

(A) t-SNE multidimensional reduction of IL-17+ lymphocytes isolated from the lungs of WT or CCR2$^{-/-}$ mice at 5 dpi (H1N1 single infection). **(B)** Quantification of the four distinct IL-17 producing populations identified in **(A). (C)** Representative flow plots showing percentage of either CD4+, IFNγ+ (top), or CD8+, IFNγ+ (bottom) lymphocytes in the lungs of mice infected with H1N1 for 5 d. **(D and E)** Quantification of lymphocytes from **(C)**. **(F)** WT or CCR2$^{-/-}$ mice were infected with H1N1, at 3 or 5 dpi whole lung homogenates were prepared and expression of IL-17 mRNA was determined via qRT-PCR. **(G)** WT or CCR2$^{-/-}$ mice were infected with H1N1 for 5d and then subsequently infected with MRSA, 24 h post MRSA infection, lung homogenates were prepared and expression of IL-17 transcript was determined via qRT-PCR. Statistical significance was calculated by Student's T-test (B, D, E and G) or ANOVA (F) * = $p < 0.05$, ** = $p < 0.01$, *** = $p < 0.001$, **** = $p < 0.0001$, n = 3 – 5 mice per group.

Author Manuscript Author Manuscript Author Manuscript Author Manuscript

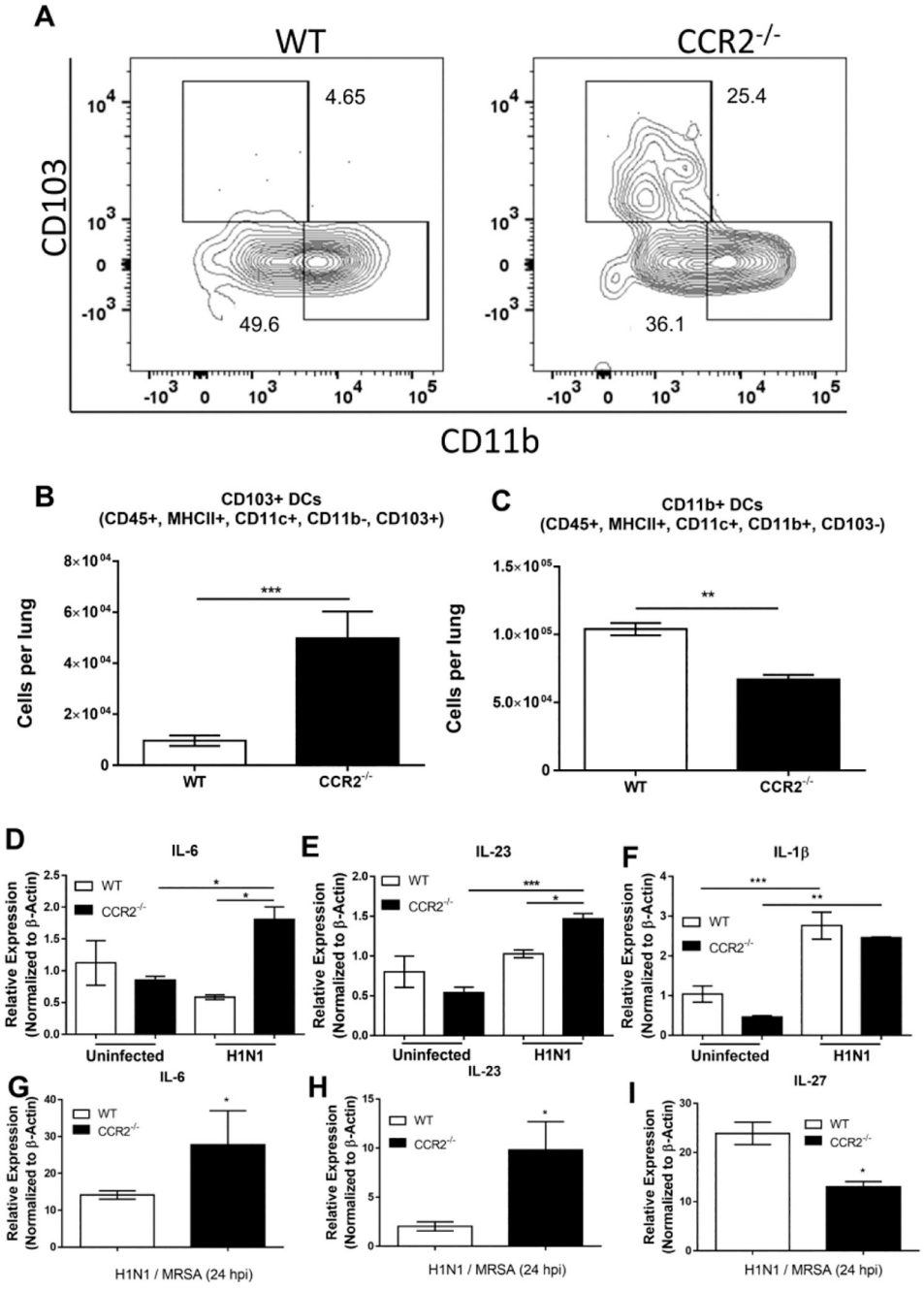

Figure 5. CCR2$^{-/-}$ mice accumulate more CD103+, pro-IL17, dendritic cells to the lungs.

(A) WT or CCR2$^{-/-}$ mice (n = 5 per group) were infected with H1N1. 5 dpi, lungs were harvested and leukocyte populations were analyzed by flow cytometry for the presence of either CD103+ or CD11b+ dendritic cells, shown are representative flow plots from two separate experiments. **(B and C)** Quantitation of flow cytometry data in (A). **(D, E and F)** WT or CCR2$^{-/-}$ mice (n = 3 per group) were infected with H1N1, 5 dpi lungs were harvested and collagenase digested. Total CD11c+ cells were isolated via magnetic sorting and analyzed by qRT-PCR for the indicated transcript. **(G, H, and I)** Mice (n = 5 – 7 per group) were infected with H1N1 for 5 days and then subsequently infected with MRSA for

Author Manuscript Author Manuscript Author Manuscript Author Manuscript

24 h. Total CD11c+ cells were isolated from collagenase digested lungs via magnetic sorting and analyzed for the indicated transcript by qRT-PCR. Statistical significance was calculated using ANOVA (D, E and F) or Student's t-test (G, H, and I), * = $p < 0.05$, ** = $p < 0.01$, *** = $p < 0.001$.

Author Manuscript Author Manuscript Author Manuscript Author Manuscript

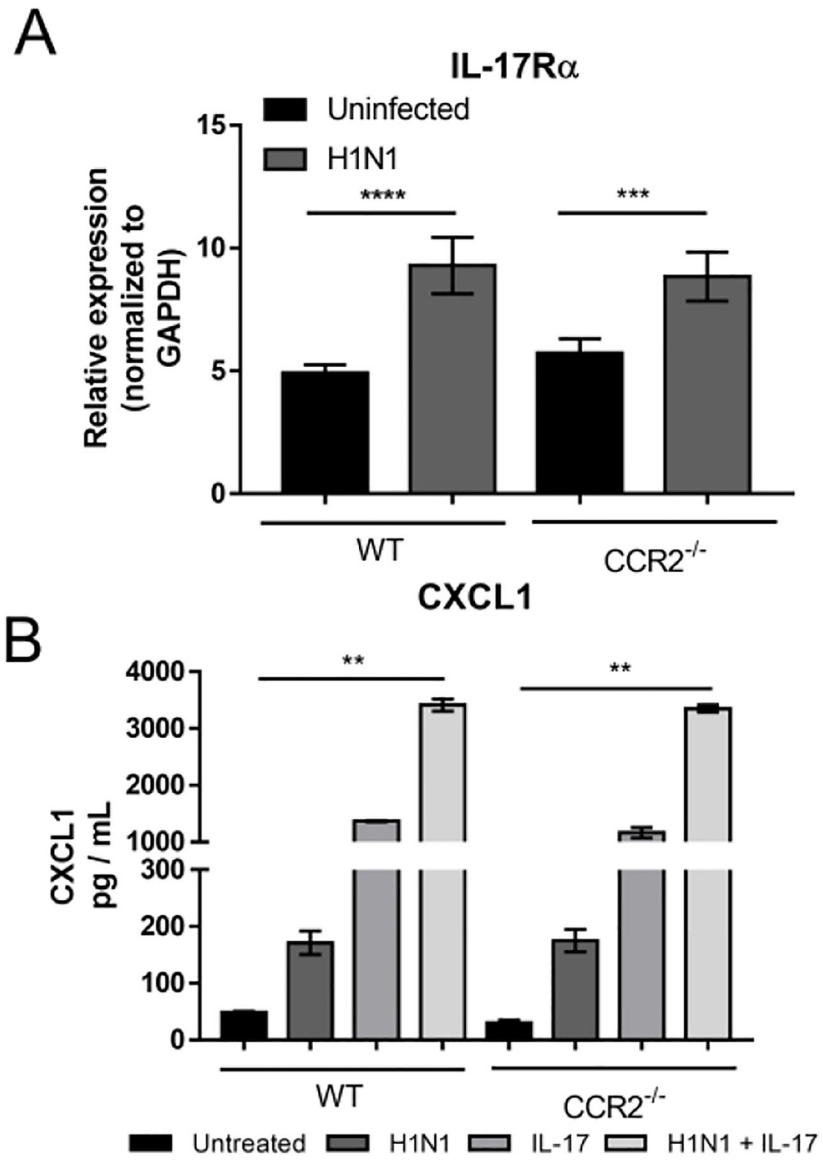

Figure 6. Isolated Alveolar Epithelial Cells express IL-17 receptor and secrete CXCL1 in response to both IL-17 stimulation and H1N1 infection.

(A) Type II alveolar epithelial cells were isolated from either WT or CCR2$^{-/-}$ mice and infected with H1N1 (MOI = 0.01) or left uninfected for 48 h. Total RNA was extracted and analyzed for the expression of IL-17Rα. **(B)** Type II alveolar epithelial cells were treated either with recombinant IL-17 (10 ng / mL), H1N1 (MOI = 0.01), or a combination of IL-17 and H1N1. After 48 h of treatment supernatants were analyzed for CXCL1 by ELISA. Statistical significance was determined using ANOVA (A), or Kruskal-Wallis non-parametric test (B) * = $p < 0.05$, ** = $p < 0.01$, *** = $p < 0.001$, **** = $p < 0.0001$, n = 3 – 5 biological replicates per group.

Author Manuscript Author Manuscript Author Manuscript Author Manuscript

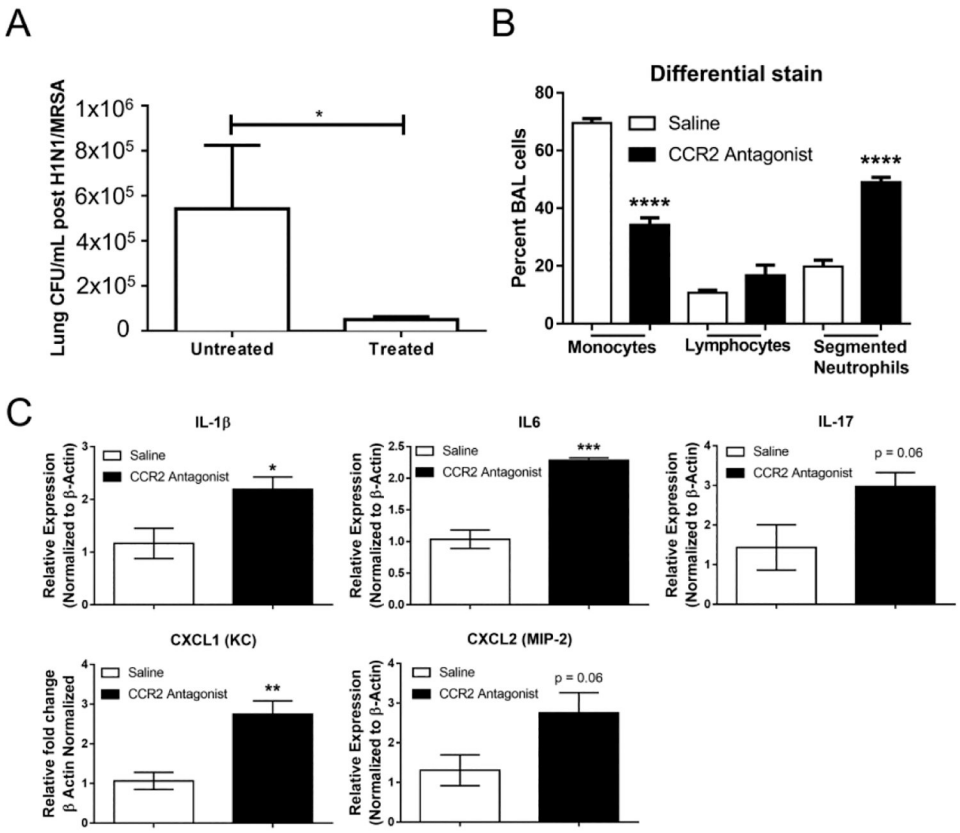

Figure 7. Mice treated with a CCR2 antagonist have altered cytokine profiles and increased IL-17 expression following H1N1 / MRSA dual infection.

WT mice were treated with CCR2 antagonist (50 μg, subcutaneously) twice daily for 5 days during infection with H1N1. After 5 days of H1N1 infection mice were subsequently infected with MRSA for 24 h. **(A)** Lung bacterial burden was calculated by serial dilution of whole lung homogenates 24 h after MRSA infection. **(B)** Following MRSA infection, BAL was performed and numbers of leukocytes were quantified by cytospin of BALF and differential stain. **(C)** Lungs were harvested and the expression of the indicated transcript was detected by qRT-PCR. Statistical significance was calculated with ANOVA (B) or Student's t-test (A and C), * = $p < 0.05$, ** = $p < 0.01$, *** = $p < 0.001$, n = 4 mice per group.

Author Manuscript Author Manuscript Author Manuscript Author Manuscript

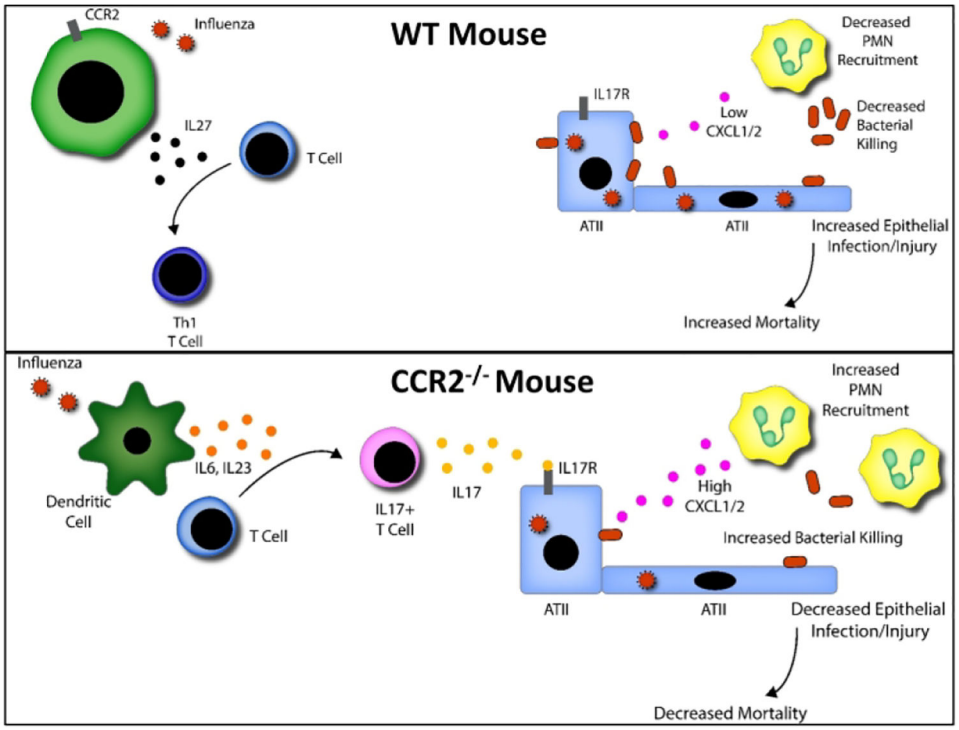

Figure 8. Proposed model for how CCR2 deficiency mediates increased neutrophil accumulation and bacterial killing.

In the absence of CCR2+ monocytes, CD103+ dendritic cells respond to influenza by producing high levels of IL-6, IL-23, and IL-1β. These pro IL-17 cytokines in conjunction with decreased production of IL-27 result in robust skewing of Th17 cells as well as IL-17 secreting γδ T-cells and iNKT cells. IL-17 can activate type II alveolar epithelial cells to produce the neutrophil recruiting chemokines CXCL1 / 2 which promote the infiltration of bactericidal neutrophils into the lung in response to a subsequent MRSA infection.

Author Manuscript

Author Manuscript

Author Manuscript

Author Manuscript

Table I.

Primers and probes used for qRT-PCR

Gene Name		Primer Sequence
IL-17A	Forward	5′-CCGCAATGAAGACCCTGATAG-3′
	Reverse	5′-GCTTTCCCTCCGCATTGA-3′
	Probe	5′-GGGAAGCTCAGTGCCGCCAG-3′
CXCL1	Forward	5’-GCGCCTATCGCCAATGAG-3’
	Reverse	5’-GCAACACCTTCAAGCTCTGGAT-3’
	Probe	5’-TGCCTGCAGACCATGGCTGGG-3’
CXCL2	Forward	5’-CCTGCCAAGGGTTGACTTCA-3’
	Reverse	5’-CCTTGAGAGTGGCTATGACTTCTG-3’
	Probe	5’-CGCCCCCAGGACCCCACTG-3’
IL-6	Forward	5’-GACTTCCATCCAGTTGCCTTCT-3’
	Reverse	5’-CTGTTGGGAGTGGTATCCTCTGT-3’
	Probe	5’-TGACAACCACGGCCTTCCCTA-3’
IL-23	Forward	5’-CTCCCTACTAGGACTCAGCCAACT-3’
	Reverse	5’-ACTCAGGCTGGGCATCTGTT-3’
	Probe	5’-AGCCAGAGGATCACCCCCGGG-3’
IL-27	Forward	5’-AGGGAATTCACAGTCAGCCT-3’
	Reverse	5’-AGATTCAGCAAAGCTGTGGA-3’
	Probe	5’-CCTTGCCAGGAAGCTGCTCTCTG-3’
IL-1β	Forward	5’-GAGCCCATCCTCTGTGACTCA-3’
	Reverse	5’-GTTGTTCATCTCGGAGCCTGTAG-3’
	Probe	5’-AACCTGCTGGTGTGTGACGTTCCCA-3’